



Progressive stirred freeze-concentration of ethanol-water solutions

M. Osorio ^a, F.L. Moreno ^b, M. Raventós ^c, E. Hernández ^c, Y. Ruiz ^{b,*}

^a Master in Design and Process Management, Universidad de La Sabana, Campus Universitario del Puente del Común, Km 7 Autopista Norte de Bogotá, Chía, Cundinamarca, Colombia

^b Agroindustrial Process Engineering, Universidad de La Sabana, Campus Universitario del Puente del Común, Km 7 Autopista Norte de Bogotá, Chía, Cundinamarca, Colombia

^c Agri-Food Engineering and Biotechnology Department, Universidad Politécnica de Cataluña (UPC) C/Esteve, Terradas, 8, 08860, Castelldefels, Barcelona, Spain

ARTICLE INFO

Article history:

Received 6 October 2017
Received in revised form
14 December 2017
Accepted 28 December 2017
Available online 2 January 2018

Keywords:

Freeze concentration
Ethanol
Response surface
Dimensionless analysis

ABSTRACT

Progressive freeze-concentration is a technology to separate water from solutions by freezing. In the present investigation, ethanol-water solutions were freeze-concentrated by the progressive stirred technique. The freezing stage was carried out in a stirring vessel. Solute recovery by the fractionated thawing of ice was also studied. The effects of stirring speed (500, 1000, and 2000 rpm), initial concentration of the solution (3%, 5%, and 8% ethanol), and temperature of the thawing stage (0, 10, and 20 °C) on the solute yield and average distribution coefficient were determined using response surface analysis. The ethanol concentration was found to have increased by 1.3 and 2.1 times at the end of the freeze concentration process. It was found that the initial concentration had a significant effect on the distribution coefficient. In addition, the average yield was increased by 28% by fractionated thawing. Subsequently, a non-dimensional analysis of the distribution coefficient was developed to yield a model to predict the distribution coefficient as a function of the Reynolds number, the relationship between the average ice growth rate and the stirring speed, the agitator diameter, and the liquid fraction. This technique proved to be valid with respect to the concentration of ethanol-water solutions, with better yields being obtained at low initial concentrations. This model is the first of its kind to describe the ethanol-water interaction in agitated freeze-concentration systems.

© 2018 Elsevier Ltd. All rights reserved.

1. Introduction

Freeze-concentration (FC) is a technique defined as a method to remove water from solutions by freezing until the formation and separation of ice crystals occurs. In this way, it is possible to obtain a product of greater concentration than the initial solution while preserving its quality (Sánchez et al., 2009). In general, there are three types of FC: suspension, block and film FC. The first is the most used in the industry for its high efficiencies, although it is associated with high operating and investment costs (Miyawaki et al., 2005; Auleda et al., 2011); which is why the researchers have looked for ways to make other techniques improve their performance (Moreno et al., 2014a; Moreno et al., 2014b).

Film freeze-concentration is an FC method, in which unidirectional crystallization of the water present in the solution takes place. In this technique, a single layer grows while being adhered to

the walls of the heat exchange surface. The solution is concentrated as it is circulated on the surface of the formed ice, which grows layer by layer. Due to the formation of a single ice layer, separation of the concentrated solution is facilitated (Liu et al., 1997; Miyawaki et al., 2016a; Miyawaki et al., 2016b; Miyawaki et al., 2005; Sánchez et al., 2009). Film FC can be classified into two types: plate FC (also called falling film) and progressive FC, as proposed by (Sánchez et al., 2009, 2011). The main difference between the two techniques is the geometry of the equipment used for the formation of crystals; the falling film FC uses a plate whereas in the progressive FC, concentration of the solute occurs at the bottom or on the walls of a tank or pipe (Sánchez et al., 2009). Further, the progressive FC equipment can be classified into two types based on their design – vertical progressive FC and tubular progressive FC (Miyawaki et al., 2005, 2015; Miyawaki and Kitano, 2015; Miyawaki et al., 2016a,b).

Agitated tanks are used for vertical progressive FC; the growth of a single ice crystal occurs at the base of the tank while it is submerged at a specific velocity in the refrigerant (Miyawaki et al., 2012). On the other hand, a tubular progressive FC consists of two

* Corresponding author.

E-mail address: ruth.ruiz@unisabana.edu.co (Y. Ruiz).

Nomenclature			
X_{s0}	Ethanol mass fraction in the initial solution (w/w)	μ	Solution viscosity (kg/ms)
X_{sice}	Ethanol mass fraction in ice (w/w)	\bar{K}_{app}	Average distribution coefficient (dimensionless)
X_{sliq}	Ethanol mass fraction in the freeze-concentrated liquid fraction (w/w)	Y	Solute yield (dimensionless)
m_{sliq}	Solute mass in the liquid fraction (kg)	CI	Concentration index (dimensionless)
m_{s0}	Solute mass in the initial solution (kg)	\bar{v}_{ice}	Average ice growth rate ($\mu\text{m/s}$)
m_{ice}	Mass of the ice sheet (kg)	f	Liquid fraction (dimensionless)
m_{liq}	Collected liquid mass (kg)	Ac	Area under the Y vs. f curve (dimensionless)
m_0	Initial mass (kg)	D_a	Diameter of the agitator (m)
ρ_{ice}	Ice density (kg/m^3)	N	Stirring speed (rps)
ρ_w	Water density (kg/m^3)	r	Vessel radius (m)
ρ_{et}	Ethanol density (kg/m^3)	t	Time of freezing (h)
ρ	Solution density (kg/m^3)	h	Ice layer height (m)
μ_w	Water viscosity (kg/ms)	T_H	Heating temperature ($^{\circ}\text{C}$)
μ_{et}	Ethanol viscosity (kg/ms)	C_0	Initial concentration (w/w)
		V_a	Stirring speed (rpm)

connected tubes; the solution circulates inside the tube while the refrigerant circulates outside, thus generating a solid phase on the inner walls and the concentrated solution flows through the ring that has not yet frozen (Miyawaki et al., 2005). Both techniques have delivered promising results using which it has been possible to demonstrate that both geometries are efficient. In the case of tubular progressive FCs, their high efficiency and ease of scaling is emphasized while in the case of vertical progressive FCs, it has been possible to obtain crystals of high purity (Miyawaki et al., 2016a,b). Recently, there was a report on hybrid equipment (Ojeda et al., 2017), which functions as a vertical progressive FC but manages to generate the ice film not only at the bottom but also on the inner walls of the tank, similar to a progressive tubular FC. One of the most important challenges faced by progressive FCs is in increasing the solute recovery (increased separation efficiency) as ice tends to grow with impurities. One strategy to increase the recovered amount is to apply controlled thawing to ice after the FC process, similar to what was done during block FC, also known as freeze-thaw process (Robles et al., 2016). Controlled thawing is usually performed on other equipment than those used to make the progressive FC (Miyawaki et al., 2012; Moreno et al., 2014b). Therefore, research is being conducted to design hybrid equipment that allows high separation efficiencies, easy scalability, and allows the controlled recovery of solutes within the same unit.

Progressive FC has been used to recover solutes from products such as wine must (Miyawaki et al., 2016a,b; Hernández et al., 2010), ethanol–water solutions (Haizum et al., 2015), juices (Miyawaki et al., 2016a,b), and coffee extracts (Gunathilake et al., 2014). The comprehension of ethanol – water solutions is useful for the application of FC to alcohol-containing matrices, such as wines or beers, which present concentration difficulties due to the loss of ethanol and volatile components related to the flavor of the drinks. A water ethanol mixture has a crystallizing line and a melting line that are separated, and thus it can exist together both liquid and solid phases (Kuwahara and Ohkubo, 2010). This condition makes the ethanol water mixtures favorable to be separated by freeze concentration techniques, in a temperature range between 0 and -70°C , according to the phase diagram proposed by (Ohkubo et al., 1997).

The objective of this work was to evaluate a progressive FC technique that combines elements of vertical and tubular progressive FCs and allows us to recover ice in the same equipment; this process will be called progressive stirred freeze-concentration

(PSFC) assisted by fractionated thawing. Ethanol–water model solutions were used to study the technique and the effect of initial concentration and stirring speed during the PSFC process on the average distribution coefficient and solute yield were determined. At the same time, a non-dimensional analysis was performed to propose an empirical mathematical model that allows us to calculate the classic variables of the FC in the proposed technique.

2. Materials and methods

2.1. Materials

Ethanol–water solutions were prepared from distilled water and commercial grade ethanol (Quimics Dalmau, Barcelona, Spain) with an initial concentration of 93.3% (w/w) ethanol.

2.2. Methods

The effect of stirring speed (V_a) and initial concentration (C_0) on the concentration of ethanol in the PSFC equipment was studied. Similarly, the effect of thawing temperature (T_H) on the recovery of solutes was also studied. A freezing temperature of -15°C was defined for the initial concentration interval studied. This condition avoids a fast freezing that can lead to the occlusion of solutes, and also allows a desirable average freezing rate, according to those reported in literature (Nakagawa et al., 2010; Moreno et al., 2014b; Petzold et al., 2016). All the FC tests were performed for 1 h.

The concentration of ethanol in each of the samples was analyzed using an electronic densimeter (DMA 35, Anton Paar) capable of reading ethanol concentration data in terms of percentage weight/weight, percentage volume/volume, density, and degrees Brix.

2.2.1. Freeze-concentration protocol

The tests were performed in the freeze-concentration equipment, similar to the one shown in Fig. 1. In the receiving tank (1), 1400 g of a previously refrigerated sample was placed; the sample was held until it reached a temperature of approximately 0°C in a cooler. The tank, which has a total height of 24 cm and diameter of 11 cm is made of AISI 304 stainless steel, and has an outer jacket (3) to allow the cooling liquid to flow; the cooling liquid is composed of a mixture of ethylene glycol and water (53% w/w) circulating in the thermostatic bath (4) equipped with a temperature controller (6).

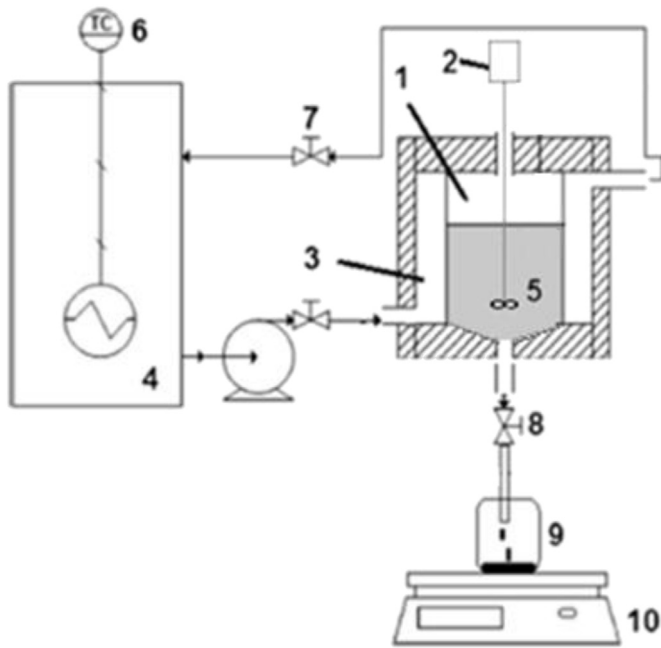


Fig. 1. Experimental set up of the PSFC process.

The tank has an outer covering of an insulating material to prevent the transfer of heat with the environment. The routing of the said flows was controlled by a system of pumps and valves (7). Due to the arrangement of the cooling jackets, the tank allows the formation of an ice film on the side walls only; a discharge cone at the bottom allows the liquid to flow out (8). The height of the solution inside the tank was 20 cm.

The solutions were agitated with a turbine rotor (5), which has 3 blades of 3 cm of length, located at 21.5 cm from the top. A mechanical stirrer (2) (RGL-100, Heidolph Instruments, Germany) equipped with a speed control system (PCE-DT62, PCE Deutschland GmbH, Germany) with 0.05% precision and 0.1 RPM resolution was used to stir the contents of the tank.

For all the tests, the refrigerant was brought to a stable processing temperature of $-15\text{ }^{\circ}\text{C}$. After that, the solution was added to the process tank. The stirring speed was defined and the FC process was then carried out for 1 h. At the end of that time, the concentrated liquid (9) was removed and weighed (10). The concentration of ethanol was measured in both the concentrated liquid and the ice obtained.

2.2.2. Thawing protocol

After the concentrated liquid has been retired, the thawing stage begins. During the controlled thawing process for the recovery of solutes from ice, the temperature of the thermostatic bath was adjusted as needed for the test in order to recover the samples in receiving containers (10). Using an analytical balance (KERN, Germany) (11), 10% of the total weight of the block was collected in each container.

2.2.3. Experimental design

A factorial design with two factors at three levels was applied for the FC tests; the stirring speeds were varied between 500, 1000, and 2000 rpm and the initial concentration of ethanol was varied between 3%, 5%, and 8% w/w. All the tests were performed in triplicate.

To analyze the controlled thaw stage, each sample was evaluated at a thawing temperature (T_H) (0, 10, and $20\text{ }^{\circ}\text{C}$).

2.2.4. Data analysis

2.2.4.1. Average distribution coefficient (\bar{K}_{app}). The average distribution coefficient, \bar{K}_{app} , represents an average ratio between the concentration of solute in the ice and the concentration of solute in the liquid phase at the end of each test (Moreno et al., 2014a; Miyawaki et al., 2012). It can be determined as shown in equation 1

$$\bar{K}_{app} = \frac{X_{s\ ice}}{X_{s\ liq}} \quad (1)$$

where $X_{s\ ice}$ is the solute concentration in the ice sheet (w/w) and $X_{s\ liq}$ is the solute concentration in the freeze concentrated liquid (w/w).

2.2.4.2. Solute yield (Y). The solute yield was used to analyze the rate of solute recovery by PSFC; it is defined as the mass of solute in the liquid fraction divided by the initial total mass of the solute (Nakagawa et al., 2010; Moreno et al., 2013). The solute yield can be determined as shown in equation 2

$$Y = \frac{m_{s\ liq}}{m_{s\ 0}} \quad (2)$$

where $m_{s\ liq}$ is the mass of solute in the liquid phase and $m_{s\ 0}$ is the initial solute mass. The obtained yield was used for both the PSFC (Y_{FC}) and thawing stage (Y_{TS}).

2.2.4.3. Concentration index (CI). The concentration index is a variable used to evaluate the increase in concentration at the end of the FC process. It is a relation between the final concentration of the solute in the concentrated liquid and the initial concentration of the sample, as shown in equation (3).

$$CI = \frac{X_{s\ liq}}{X_{s\ 0}} \quad (3)$$

2.2.4.4. Average ice growth rate (\bar{v}_{ice}). The average ice growth rate is calculated at the end of the operation and takes into account the ice conditions (mass, concentration, and density), in addition to the area of heat transfer and time of operation, as shown in equation (4) (Chen et al., 1998; Moreno et al., 2014a). Chen and Chen (2000) showed the application of this variable for a falling film FC equipment. Equation (4) shows the application of the average ice growth rate for a stirred tank, where r is the vessel radius and h is the height of ice layer, both in meters. m_{ice} is the mass of the ice obtained (kg), $X_{s\ ice}$ is the mass concentration of ethanol in ice, and ρ_{ice} is the density of ice.

$$\bar{v}_{ice} = \frac{r - \sqrt{r^2 - \frac{m_{ice}(1-X_{s\ ice})}{\rho_{ice} h \pi}}}{t} \quad (4)$$

2.2.4.5. Liquid fraction (f). The liquid fraction, f , is defined as the ratio between the concentrated liquid mass and the initial total mass (Nakagawa et al., 2010; Miyawaki et al., 2012). It is used in controlled thawing trials to follow the development of the solute recovery process (Gulfo et al., 2014).

2.2.4.6. Area under the Y vs. f curve (A_c). The graph of Y vs. f represents the percentage of solute recovered from the initial solution in each thawed liquid fraction (Nakagawa et al., 2010). The area under the curve can be used as a parameter to analyze the efficiency of the separation process and to examine the effect of the

factors studied (Moreno et al., 2014b). The area under the curve of Y vs. f was obtained by a spline regression procedure, according to (Moreno et al., 2014b).

2.2.5. Dimensionless model

A non-dimensional analysis was performed for the PSFC using the Vaschy–Buckingham π theorem (Curtis et al., 1982; Baker et al., 1991) to develop a model for \bar{K}_{app} , which acts as a representative of the geometry of the equipment studied. Within the factors chosen to develop the model, the physical properties of the solutions were taken into account as well as the parameters of operation and equipment design (Delaplace et al. 2015a, 2015b). Two of the studied factors were the density (ρ) and viscosity (μ) of the mixture; these parameters are important when analyzing transport phenomena. In addition, several researchers identified that the average growth rate of ice is an important variable in obtaining the purest ice (Chen et al., 1998; Moreno et al., 2014a). The other factor employed in the model is f ; it is used in various FC techniques as an operation parameter (Nakagawa et al., 2010; Miyawaki et al., 2012; Moreno et al., 2014b). Finally, the initial concentration was taken into account because it has been confirmed that it is a variable with a significant effect on the average distribution coefficient (Moreno et al., 2014b; Petzold and Aguilera, 2009; Raventós et al., 2007).

At the same time, the stirring speed and the agitator diameter were considered as they are classical parameters for any process carried out in a stirred tank (Michell and Perry, 1964). The model for the progressive stirred FC is shown in equation (5).

$$\bar{K}_{app} = f(f, C_0, \rho, \mu, N, \bar{v}_{ice}, D_a) \quad (5)$$

The density of the solution was calculated using equations (6)–(8). Similarly, the viscosity was calculated using equations (9)–(11). Equations (7), (8), (10) and (11) were simulated in the ASPEN PLUS software, using the NRTL thermodynamic model. Equations (6) and (9) were used (Moreno et al., 2014a) with coffee solutions and were shown to be suitable for modeling density and viscosity near the freezing temperatures.

$$\frac{1}{\rho} = \frac{X_s liq}{\rho_{et}} + \frac{(1 - X_s liq)}{\rho_w} \quad (6)$$

$$\rho_{et} = 807,66 - 0,8249T - 0,0003T^2 \left(\frac{kg}{m^3} \right) \quad (7)$$

$$\rho_w = 1002,7 - 0,2712T - 0,0015T^2 \left(\frac{kg}{m^3} \right) \quad (8)$$

$$\ln \mu = X_s liq \ln(\mu_{et}) + (1 - X_s liq) \ln(\mu_w) \left(\frac{kg}{ms} \right) \quad (9)$$

$$\mu_{et} = 0,0017 - 0,00004T - 0,000002T^2 \left(\frac{kg}{ms} \right) \quad (10)$$

$$\mu_w = 0,0018 - 0,00003T - 0,0000008T^2 \left(\frac{kg}{ms} \right) \quad (11)$$

The density data calculated from equation (6) was compared with experimental data on the density of ethanol-water solutions reported in the International Organization of Legal Metrology (OIML) alcohol grade conversion tables (OIML, 1972). The densities of the water-ethanol blends (20% alcohol) were compared at temperatures of 0, -5, and -10 °C. The correlation coefficient, R^2 , between the data predicted by the equations and the experimental

data had a value of 0.999. The results calculated using equations (10) and (11) were contrasted with the data reported elsewhere (Nikumbh and Kulkarni, 2013) at a temperature of 20 °C.

2.3. Statistical analysis

A response surface analysis methodology was developed to find the optimum operating points for the PSFC and for the recovery of solutes by controlled thawing, with a significance level of 95%. One-way analysis of variance (ANOVA) was applied to the results followed by a LSD test with a significance level of 95%.

To obtain the parameters of the model, it was linearized and later linear regression was performed with Stepwise to determine which variables had a significant effect on the model and using which the R^2 of the model was maximized. The assumptions of the linear regression model were validated and the residuals were evaluated through a Shapiro-Wilks test for normality; the variance was tested for homogeneity and presence of atypical and influential data. All statistical analyses were conducted using the SAS 9.2 software.

3. Results and discussion

3.1. Progressive stirred FC

Twenty-seven tests were carried out on the progressive stirred freeze-concentration equipment. The obtained \bar{K}_{app} values were in the range of 0.17–0.6 with an average value of 0.42, similar to those obtained in other FC systems with ethanol and water mixtures (Haizum et al., 2015), in coffee extracts (Moreno et al., 2014a), and other food matrices such as sucrose and juice solutions (Miyawaki et al., 2005; Miyawaki et al., 2016a,b; Gulfo et al., 2014; Auleda et al., 2011). The results are shown in Table 1.

Table 1 shows the results of \bar{K}_{app} and the average crystal growth rate at each of the studied conditions. The lowest values were obtained when the initial concentration of ethanol was low. This may be because the viscosity increases at high concentrations, which hinders mass transfer (Moreno et al., 2014a; Moreno et al., 2014b), and induces a tendency for the formation of dendritic ice that generates occlusions, when the solute concentration is high (Robles et al., 2016). In the same way, higher values of CI were obtained at lower initial concentrations, and are comparable to those reported in other samples as coffee extract (Moreno et al., 2014c). However, at higher initial concentration the CI is lower in comparison than those reported in other samples, such as sucrose and juice solutions (Miyawaki et al., 2005; Miyawaki et al., 2016a,b; Gulfo et al., 2014; Auleda et al., 2011). When the initial concentration increases, there will be a greater molecular interaction, which can cause a lower diffusion of the solute through the formed ice film, decreasing the CI (Petzold and Aguilera, 2009). This effect will be more evident in the studied sample, since hydrogen bonds of water are reinforced by addition of ethanol molecules (Li et al., 2017).

The average growth rate of the ice crystals is in the range of 3.13 $\mu\text{m/s}$ to 4.82 $\mu\text{m/s}$. At similar ice growth rates, freeze-concentration was reported for solutions of sucrose and coffee (Moreno et al., 2014a; Moreno et al., 2014b; Nakagawa et al., 2010; Chen and Chen, 2000). An ANOVA procedure was performed on the mean ice growth rate for each of the initial concentrations; at a confidence interval of 5%, there was no significant difference between the ice growth rates at different initial concentrations. One possible explanation for this behavior may be the use of a constant freezing temperature for all the tests. On the other hand, the value of \bar{K}_{app} decreases with an increase in the stirring speed at each initial concentration, but not significantly in the studied interval. The largest drops in \bar{K}_{app} with respect to the stirring speed occurred at low initial concentrations of the solution.

Table 1
Results obtained for the PSFC for different solutions.

C ₀	V _A	Y	IC	\bar{v}_{ice} μm/s	\bar{K}_{app}	f	X _{S liq}	X _{S ice}	Liquid volumen (L)	Ice volumen (L)
0,03	500	0,38 ± 0,02	0,05 ± 0,00	0,01 ± 0,00	0,85 ± 0,03	0,54 ± 0,03	0,62 ± 0,03	1,76 ± 0,06	4,30 ± 0,23	0,32 ± 0,03
0,03	1000	0,38 ± 0,02	0,05 ± 0,00	0,01 ± 0,00	0,85 ± 0,03	0,54 ± 0,03	0,65 ± 0,04	1,92 ± 0,08	4,30 ± 0,20	0,25 ± 0,05
0,03	2000	0,33 ± 0,01	0,06 ± 0,00	0,01 ± 0,00	0,92 ± 0,01	0,48 ± 0,01	0,67 ± 0,08	2,06 ± 0,23	4,74 ± 0,09	0,23 ± 0,09
0,05	500	0,43 ± 0,01	0,07 ± 0,00	0,03 ± 0,00	0,79 ± 0,01	0,60 ± 0,01	0,56 ± 0,02	1,49 ± 0,04	3,86 ± 0,09	0,45 ± 0,03
0,05	1000	0,38 ± 0,04	0,08 ± 0,00	0,03 ± 0,00	0,85 ± 0,06	0,54 ± 0,06	0,46 ± 0,05	1,66 ± 0,16	4,21 ± 0,36	0,42 ± 0,08
0,05	2000	0,36 ± 0,02	0,09 ± 0,01	0,03 ± 0,00	0,89 ± 0,03	0,51 ± 0,03	0,52 ± 0,04	1,82 ± 0,26	4,41 ± 0,20	0,35 ± 0,05
0,08	500	0,48 ± 0,02	0,10 ± 0,00	0,05 ± 0,00	0,71 ± 0,03	0,69 ± 0,03	0,54 ± 0,03	1,36 ± 0,02	3,31 ± 0,18	0,52 ± 0,04
0,08	1000	0,42 ± 0,03	0,12 ± 0,00	0,05 ± 0,00	0,81 ± 0,05	0,59 ± 0,05	0,48 ± 0,05	1,51 ± 0,02	3,80 ± 0,29	0,48 ± 0,02
0,08	2000	0,43 ± 0,01	0,11 ± 0,00	0,05 ± 0,00	0,80 ± 0,02	0,61 ± 0,02	0,51 ± 0,04	1,47 ± 0,05	3,75 ± 0,11	0,49 ± 0,02

Response surface analysis was conducted to identify the effect of various parameters on \bar{K}_{app} and Y; the results are shown in Table 2. It was found that of the various parameter ranges studied, the initial concentration of ethanol had a significant effect on the average distribution coefficient as well as the solute yield. Conversely, neither the stirring rate nor the interactions between the initial concentration and stirring speed had a significant effect on the two response variables studied. It was found that the initial concentration of ethanol had a positive effect on the average distribution coefficient and a negative effect on the solute yield of the FC phase. This can be explained as follows. A higher concentration of solutes in the solution will generate greater occlusions in the formed ice sheet, leading to an increase in \bar{K}_{app} , which in turn causes a decrease in the yield of the recovered solutes (Moreno et al., 2014a).

For the parameter ranges studied in this work, response surface analysis indicated that an initial ethanol concentration of 3% and a stirring speed of 1300 rpm were the optimum operating points, which corresponds to the lowest concentration and a medium stirring speed; However, the stirring speed did not have a significant effect in the studied interval. Fig. 2 corroborates the expected behavior of both the variables with respect to the initial concentration. Low yields and high \bar{K}_{app} values were observed at high concentrations, which indicates a large number of occlusions in the ice.

3.2. Controlled thawing

A controlled thawing process was performed on the ice sheet to increase the value of Y obtained in the first phase of the process. During the thawing process, the solute occluded in the ice layer can be recovered by its diffusion into the drops that are melting. Controlled thawing has been tested for block FC (Moreno et al., 2013; Moreno et al., 2014b) and film FC (Miyawaki et al., 2012; Miyawaki et al., 2016a,b; Gulfo et al., 2014). In the present study, controlled thawing could be performed in the same equipment in which progressive FC was implemented. A response surface analysis of the factors V_A, C₀, and T_H was performed on the response variables Y (when CI was equal to one) and Ac; significant effects

Table 2
Significance factors of the response surface analysis of the progressive stirred FC.

Parameter	\bar{K}_{app}		Y	
	Estimator	Pr < f	Estimator	Pr < f
C ₀	15.712	0.0009 ^a	-15.764	0.0009 ^a
V _A	-0.001	0.3346	-0.0001	0.1450
C ₀ * C ₀	-107.407	0.0063	127.407	0.0017 ^a
C ₀ * V _A	0.001	0.1949	-0.0001	0.2904
V _A * V _A	5.92E-09	0.8917	8.81E-08	0.0533

^a Indicates significance with an alpha of 0.05.

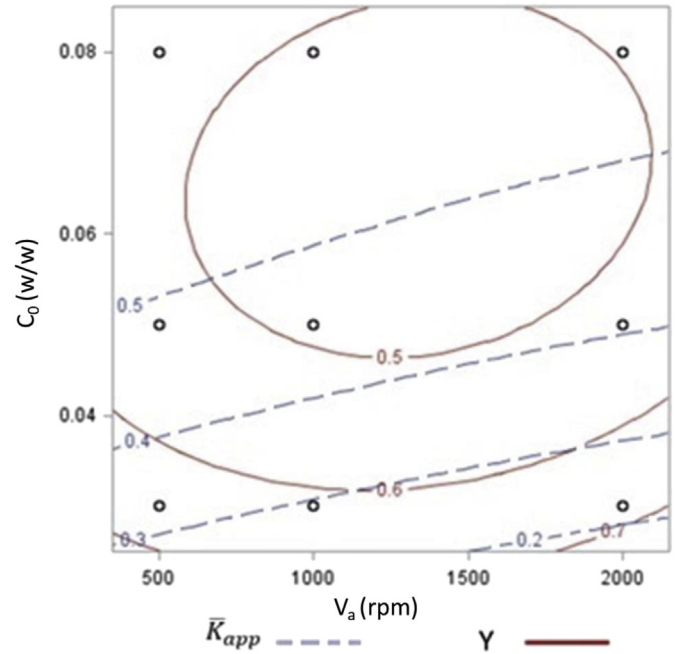


Fig. 2. Response contours of \bar{K}_{app} and Y as functions of the initial concentration and stirring speed.

were found with C₀ and T_H. The significance levels of both the variables are shown in Table 3.

Fig. 3 shows that the effect of initial concentration on the concentration index and area under the curve is negative; at a low C₀, a high CI was obtained for the first fractions recovered, in addition to reaching the CI equal to 1 to a minor fraction of thawing. Likewise, the area under the curve is high at low concentrations. As mentioned previously, low concentrations are associated with low \bar{K}_{app} values; therefore, at the beginning of the controlled thaw process, concentrated fractions can be obtained easily as well as the final fractions without any solutes. The same behavior was reported elsewhere (Moreno et al., 2013; Moreno et al., 2014b; Gulfo et al., 2014) with coffee extracts.

Table 3
Significance values from ANOVA, with an alpha of 0.05*, for controlled thawing.

Parameter	Ac		Y _{RS}	
	F value	Pr < f	F value	Pr < f
Co	19,098	3,20E-04*	7118	0,02*
V_A	1188	0,415	6137	0,945
T_H	1752	0,219	0056	0,015*

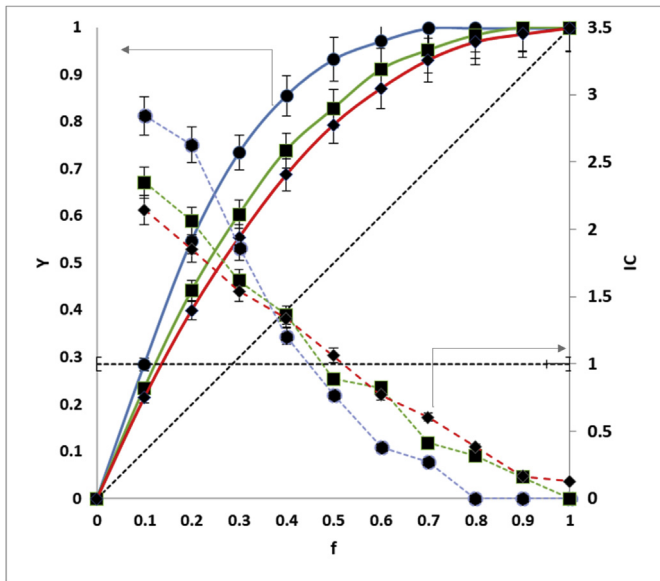


Fig. 3. Effect of initial concentration on CI (dotted line) and Ac (solid line) for the test at 2000 rpm and 0 °C. The initial concentrations were 3% (blue - ●), 5% (green - ■), and 8% (red - ◆). (For interpretation of the references to colour in this figure legend, the reader is referred to the Web version of this article.)

Fig. 4 shows that T_H had a negative effect on both the variables, similar to the results reported previously (Moreno et al., 2013). This may be because the higher the temperatures the faster the heat transfer, so the ice melts faster and it is not feasible to recover the concentrated solution trapped in the crystal structure before the melting phenomenon occurs. However, the use of low thawing temperatures during the thawing process can be associated with low mass transfer, so the solutes trapped on the ice layer will not be able to migrate to the external surface of the ice. Also, low temperatures significantly increases time of controlled thawing; to reach a CI of 1 at 0 °C, it takes about 4 h, while at 10 °C and 20 °C, 3 h and 1.5 h, respectively, were required.

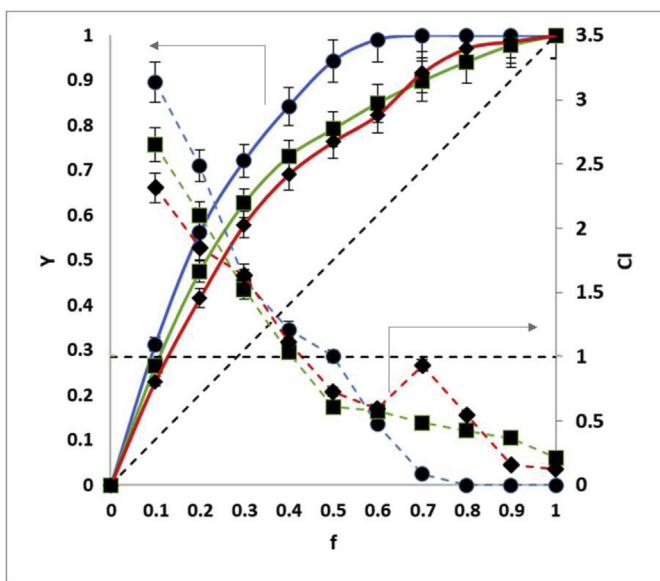


Fig. 4. Effect of thawing temperature on CI (dotted line) and Ac (solid line) at 1000 rpm and 5% ethanol concentration. The TH values were 0 °C (blue - ●), 10 °C (green - ■), and 20 °C (red - ◆). (For interpretation of the references to colour in this figure legend, the reader is referred to the Web version of this article.)

Although this equipment has a single jacket, which does not allow recovery with a counterflow system as recommended (Moreno et al., 2014b), it was possible to obtain Y values in the range of 0.59–0.98 (average value of 0.76) in the thawing stage, which are comparable to those reported for coffee (Moreno et al., 2014b). On the other hand, the Ac values were in the range of 0.72–0.96, with an average value of 0.81. A response contour plot (Fig. 5) was generated for these variables as functions of the initial concentration and the thawing temperature. Response surface analysis allowed us to calculate the optimal points for these variables at C_0 of 0.03 and T_H of 8 °C, which led to a Y value of 0.89 and Ac value of 0.8. This temperature can allow a good balance between thawing speed (heat transfer) and separation speed (mass transfer) (Moreno et al., 2013).

Equation (2) was used to calculate the total solute yield, considering that the mass of the total solute is composed of the mass of the solute obtained in the FC phase and the mass obtained during the controlled thawing stage, which was calculated using a mass balance to evaluate the amount of ethanol in the ice block once the controlled thawing process started and the yield reached at an CI equal to 1. The application of controlled thawing allowed an average total solute yield of 0.84, which is ~28% higher than that obtained with only PSFC. The application of the controlled thaw phase proved to be a viable route to increasing the solute yield, presenting a possible solution to the negative effect of increasing concentration on the Y and \bar{K}_{app} values, as it allows us to recover those solutes that were occluded during the FC stage.

3.3. Dimensionless model

A dimensionless model was developed for the PSFC without the thawing stage. For the model, the non-dimensional numbers shown in equations (13)–(15) were obtained in addition to the initial concentration. The first number obtained was the inverse of the Reynolds number for agitated tanks (Michell and Perry, 1964). The second number is a relationship between the average ice growth rate, stirring speed, and agitator diameter. The third dimensionless number is the liquid fraction. The model and its linearization are shown in equation (16) and equation (17), respectively.

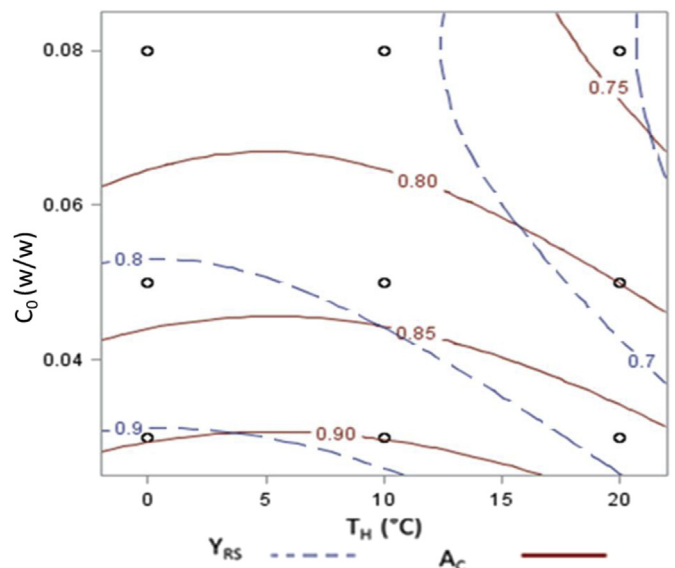


Fig. 5. Response contours of Y and Ac at 1100 rpm.

$$\pi_1 = \frac{\mu}{D_a^2 \rho N} = \frac{1}{Re} \tag{13}$$

$$\pi_2 = \frac{v_{ice}}{D_a N} \tag{14}$$

$$\pi_3 = f \tag{15}$$

$$\bar{K}_{app} = f(\pi_1, \pi_2, \pi_3, C_0) = \left(\frac{1}{Re}\right)^a \left(\frac{v_{ice}}{D_a N}\right)^b (f)^c (C_0)^d \tag{16}$$

$$\ln(\bar{K}_{app}) = a \cdot \ln\left(\frac{1}{Re}\right) + b \cdot \ln\left(\frac{v_{ice}}{D_a N}\right) + c \cdot \ln(f) + d \cdot \ln(C_0) \tag{17}$$

To determine the coefficients a, b, c, and d in the model, a linear regression model was used via the SAS maximization methodology of R²; the model shown in equation (18) was obtained, with a R² value of 0.7726. Experimental data were compared with predicted data in Fig. 6. This value indicates that the model can suitably predict \bar{K}_{app} values.

$$\bar{K}_{app} = 13131.77(Re)^{1.83} \left(\frac{v_{ice}}{D_a N}\right)^{2.07} (f)^{1.01} (C_0)^{0.93} \tag{18}$$

To determine the significance of the variables in the model, a stepwise regression analysis was performed and the results are shown in Table 4. It was found that, for the case studied, the term ln(C₀) has a significant effect.

The dimensionless number of equation (14) is very similar to the relationship proposed in the Chen & Chen model (Chen and Chen, 2000; Chen et al., 1999) for a falling film FC. It was suggested that this velocity relation is the relationship between the heat transfer phenomena, which is in turn related to \bar{v}_{ice} (Qin et al., 2009) and the mass transfer phenomena; in this case, related to the velocity, $D_a N$, of the fluid driven by the impeller of the agitated tank (Chen et al., 1998). In this way, the value of \bar{K}_{app} will decrease (greater separation efficiencies will be obtained) at lower ice crystal growth velocities and high stirring rates; thus, high mass transfer rates can be observed in the liquid phase. This behavior can be observed in Fig. 7, in which the effect of concentration is evident. This behavior has

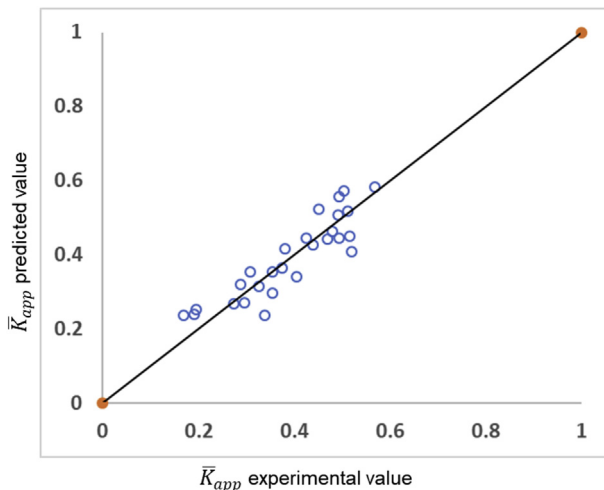


Fig. 6. Parity plot of the average distribution coefficient. Experimental vs predicted data from Eq. (18).

Table 4

Results of stepwise regression analysis and the parameters with a significant effect on the model (equation (18)).

Variable	Parameter estimator	Pr > F
Intercept	9.48279	0.2991
ln(C ₀)	0.93468	0.0020 ^a
ln(f)	1.01192	0.6701
ln($\frac{\bar{v}_{ice}}{D_a N}$)	2.07019	0.4878
ln($\frac{\mu}{D_a^2 \rho N}$)	-1.83535	0.5367

^a Indicates significance with an alpha of 0.05.

already been reported in the freeze-concentration theory and is explained as follows. At low crystal growth rates, it is feasible for the formed network to grow in an orderly manner allowing the expulsion of solutes (Robles et al., 2016; Moreno et al., 2014b; Chen et al., 1999). On the other hand, a high mass transfer rate in the liquid phase allows the elution of solutes near the ice surface in formation so that the ice grows cleaner (Haizum et al., 2015).

Another factor that appears in the model is an expression of the Reynolds number, whose behavior with respect to \bar{K}_{app} is shown in Fig. 8. \bar{K}_{app} depend mainly on the initial concentration. The effect of the stirring speed on K_{app} was inverse, but with not significance in the studied interval. This may be because in the evaluated parameter ranges, all the experimental data were found to be in the turbulent regime. Therefore, an increase in the velocity will not affect the system, similar to the case of the number of power in agitated tanks (Doran and Doran, 2013).

Finally, the influence of the initial concentration of the solution is considered; at higher concentrations, the average distribution coefficient is higher. This experimental observation is in good agreement with the available literature (Moreno et al., 2014b; Petzold and Aguilera, 2009; Raventós et al., 2007). The model proved to fulfill all the assumptions of a linear regression model and was tested using the Shapiro-Wilk method; it demonstrates a causal relationship between the chosen variables and the response variables.

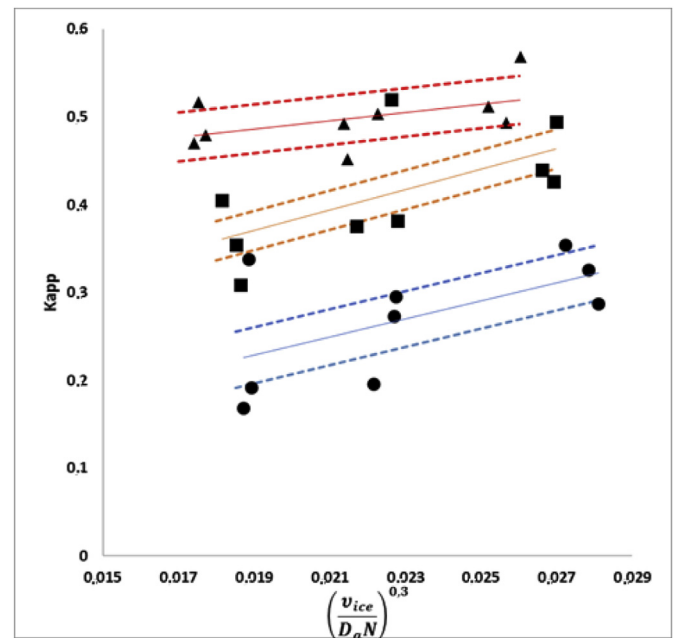


Fig. 7. Effect of $\frac{\bar{v}_{ice}}{D_a N}$ on \bar{K}_{app} . Co 3% (blue - ●), 5% (orange - ■), and 8% (red - ▲). The solid lines represent experimental data while the dotted lines represent confidence limits of 95%. (For interpretation of the references to colour in this figure legend, the reader is referred to the Web version of this article.)

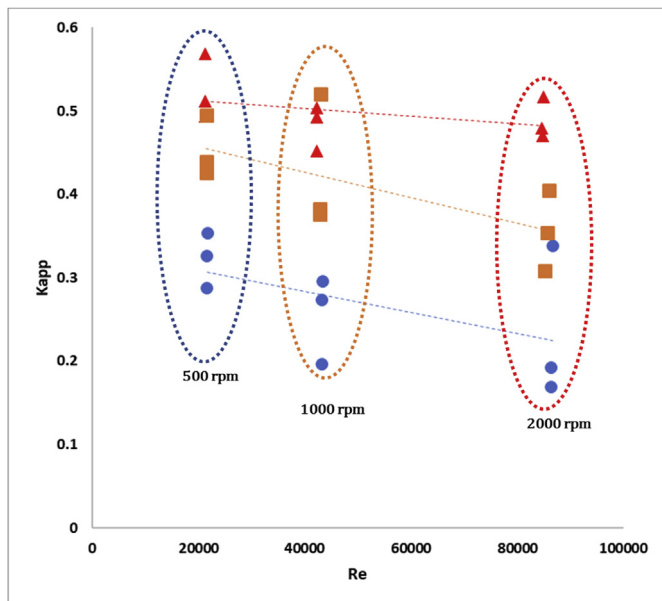


Fig. 8. Effect of Reynolds number on \bar{K}_{app} . The initial concentrations were 3% (blue - ●), 5% (orange - ■), and 8% (red - ◆). Dotted lines represent the trend of the data for each initial concentration. (For interpretation of the references to colour in this figure legend, the reader is referred to the Web version of this article.)

4. Conclusions

It was possible to freeze concentrate solutions of ethanol-water in a progressive stirred FC, thus showing the feasibility of the new technique. The initial concentration of the water-ethanol solutions was found to have a significant effect on the average distribution coefficient and solute recovery; purer ices and consequently lower \bar{K}_{app} values were obtained at low initial concentrations. It was possible to apply a controlled thawing stage to improve the recovery of the occluded ice after the PSFC process in the same equipment, thus increasing solute recovery by ~28%. Based on the concept of dimensionless modeling, a mathematical model was proposed for the \bar{K}_{app} behavior; it showed a good fit and could accurately predict \bar{K}_{app} values.

Acknowledgements

This work was supported by the ING-162-2015 project of the Faculty of Engineering of Universidad de La Sabana. The authors thank the Universidad Politècnica de Cataluña for providing support for the experimental development of the project. Further, the authors thank Dr. Edgar Benitez for providing his support in the development of the project. Ing. Manuel Osorio acknowledges support from the graduate assistance program of the Universidad de La Sabana.

References

Auleda, J.M., et al., 2011. Estimation of the freezing point of concentrated fruit juices for application in freeze concentration. *J. Food Eng.* 105 (2), 289–294. Available at: <http://www.sciencedirect.com/science/article/pii/S0260877411000999>. (Accessed 12 October 2015).

Baker, W.E., Westine, P., Dodge, F., 1991. Development of model laws from the buckingham pi theorem. In: *Similarity Methods in Engineering Dynamics: Theory and Practice of Scale Modeling*, pp. 19–31. Available at: <http://linkinghub.elsevier.com/retrieve/pii/B9780444881564500087>. (Accessed 28 May 2017).

Chen, P., Chen, X.D., 2000. A generalized correlation of solute inclusion in ice formed from aqueous solutions and food liquids on sub-cooled surface. *Can. J. Chem. Eng.* 78 (2), 312–319. Available at: <http://doi.wiley.com/10.1002/cjce.5450780205>. (Accessed 26 October 2015).

Chen, P., Chen, X.D., Free, K.W., 1999. An experimental study on the spatial uniformity of solute inclusion in ice formed from falling film flows on a sub-cooled surface. *J. Food Eng.* 39 (1), 101–105. Available at: <http://www.sciencedirect.com/science/article/pii/S0260877498001526>. (Accessed 26 October 2015).

Chen, P., Chen, X.D., Free, K.W., 1998. Solute inclusion in ice formed from sucrose solutions on a sub-cooled surface—an experimental study. *J. Food Eng.* 38 (1), 1–13. Available at: <http://www.sciencedirect.com/science/article/pii/S0260877498001125>. (Accessed 12 October 2015).

Curtis, W.D., Logan, J.D., Parker, W.A., 1982. Dimensional analysis and the pi theorem. *Lin. Algebra Appl.* 47, 117–126. Available at: <http://linkinghub.elsevier.com/retrieve/pii/0024379582902294>. (Accessed 28 May 2017).

Delaplace, G., et al., 2015a. 1 – objectives and value of dimensional analysis. In: *Dimensional Analysis of Food Process*, pp. 1–11. Available at: <http://www.sciencedirect.com.ez.unisabana.edu.co/science/article/pii/B9781785480409500016>. (Accessed 28 May 2017).

Delaplace, G., et al., 2015b. 2 – dimensional analysis: principles and methodology. In: *Dimensional Analysis of Food Process*, pp. 13–59. Available at: <http://www.sciencedirect.com.ez.unisabana.edu.co/science/article/pii/B9781785480409500028>. (Accessed 28 May 2017).

Doran, P.M., Doran, P.M., 2013. Chapter 8 – mixing. In: *Bioprocess Engineering Principles*, pp. 255–332. Available at: <http://www.sciencedirect.com.ez.unisabana.edu.co/science/article/pii/B9780122208515000083>. (Accessed 28 May 2017).

Gulfo, R., et al., 2014. Multi-plate freeze concentration: recovery of solutes occluded in the ice and determination of thawing time. *Food Sci. Technol. Int.* 20 (6), 405–419. Available at: <http://www.ncbi.nlm.nih.gov/pubmed/23785068>. (Accessed 10 March 2016).

Gunathilake, M., et al., 2014. Flavor retention in progressive freeze-concentration of coffee extract and pear (La France) juice flavor condensate. *Food Sci. Technol. Res.* 20 (3), 547–554. Available at: <http://jlc.jst.go.jp/DN/JST/JSTAGE/fstr/20.547?lang=en&from=CrossRef&type=abstract>. (Accessed 15 June 2016).

Haizum, S., et al., 2015. Fractional freezing of ethanol and water mixture. *J. Technol.* 7, 49–52.

Hernández, E., et al., 2010. Freeze concentration of must in a pilot plant falling film cryoconcentrator. *Innovat. Food Sci. Emerg. Technol.* 11 (1), 130–136. Available at: <http://www.sciencedirect.com/science/article/pii/S146685640900109X>. (Accessed 5 July 2015).

Kuwahara, K., Ohkubo, H., 2010. Crystal growth of water ethanol mixture. In: 2010 International Symposium on Next-generation Air Conditioning and Refrigeration Technology, pp. 17–19. Available at: [file:///C:/Users/Manuel/Downloads/CRYSTAL GROWTH OF WATER ETHANOL MIXTURE.pdf](file:///C:/Users/Manuel/Downloads/CRYSTAL%20GROWTH%20OF%20WATER%20ETHANOL%20MIXTURE.pdf). (Accessed 21 August 2015).

Li, F., et al., 2017. Study of Hydrogen Bonding in Ethanol-water Binary Solutions by Raman Spectroscopy. Available at: https://ac.els-cdn.com/S1386142517307060/1-s2.0-S1386142517307060-main.pdf?_tid=43497850-ceca-11e7-8461-00000aab0f6c&acdnat=1511275556_a38082cef31751509239d38399d5802d. (Accessed 21 November 2017).

Liu, L., Miyawaki, O., Nakamura, K., 1997. Progressive freeze-concentration of model liquid food. *Food Sci Technol. Int. Tokyo* 3 (4), 348–352. Available at: https://www.jstage.jst.go.jp/article/fsti9596t9798/3/4/3_4_348/_pdf. (Accessed 14 June 2016).

Michell, S.J., Perry, M., 1964. *Fluid and Particle Mechanics*.

Miyawaki, N., Kitano, S., 2015. Progressive Freeze-concentration System. Available at: http://worldwide.espacenet.com/publicationDetails/biblio?CC=JP&NR=5656037B1&KC=B1&FT=D&ND=3&date=20150121&DB=EPODOC&locale=en_EP.

Miyawaki, N., Koyanagi, T., Kitano, S., 2015. Production Method and System for Fruit Wine Using Surface Progress Freeze Concentration Method. Available at: http://worldwide.espacenet.com/publicationDetails/biblio?CC=JP&NR=2015204777A&KC=A&FT=D&ND=3&date=20151119&DB=EPODOC&locale=en_EP.

Miyawaki, O., Omote, C., et al., 2016a. Integrated system of progressive freeze-concentration combined with partial ice-melting for yield improvement. *J. Food Eng.* 184, 38–43.

Miyawaki, O., Gunathilake, M., et al., 2016b. Progressive freeze-concentration of apple juice and its application to produce a new type apple wine. *J. Food Eng.* 171, 153–158.

Miyawaki, O., et al., 2005. Tubular ice system for scale-up of progressive freeze-concentration. *J. Food Eng.* 69 (1), 107–113.

Miyawaki, O., Kato, S., Watabe, K., 2012. Yield improvement in progressive freeze-concentration by partial melting of ice. *J. Food Eng.* 108 (3), 377–382. Available at: <http://www.sciencedirect.com/science/article/pii/S0260877411004961>. (Accessed 26 October 2015).

Moreno, F.L., Hernández, E., et al., 2014c. A process to concentrate coffee extract by the integration of falling film and block freeze-concentration. *J. Food Eng.* 128, 88–95. Available at: <https://doi.org/10.1016/j.jfoodeng.2013.12.022>.

Moreno, F.L., Raventós, M., et al., 2014a. Behaviour of falling-film freeze concentration of coffee extract. *J. Food Eng.* 141, 20–26. Available at: <https://doi.org/10.1016/j.jfoodeng.2014.05.012>.

Moreno, F.L., Raventós, M., et al., 2014b. Block freeze-concentration of coffee extract: effect of freezing and thawing stages on solute recovery and bioactive compounds. *J. Food Eng.* 120 (1), 158–166. Available at: <https://doi.org/10.1016/j.jfoodeng.2013.07.034>.

Moreno, F.L., et al., 2013. Effect of separation and thawing mode on block freeze-concentration of cvfvooffee brews. *Food Bioprod. Process.* 91 (4), 396–402. Available at: <https://doi.org/10.1016/j.fbp.2013.02.007>.

Nakagawa, K., Maebashi, S., Maeda, K., 2010. Freeze-thawing as a path to concentrate aqueous solution. *Separ. Purif. Technol.* 73 (3), 403–408. Available at: <http://www.sciencedirect.com/science/article/pii/S1383586610001899>. (Accessed 17 September 2015).

- Nikumbh, A., Kulkarni, G., 2013. Density and viscosity study of binary mixtures of ethanol–water at different temperatures. *Sci. J. Pure Appl. Chem.*, ISSN 2276–6308. Available at: <http://www.sjpub.org>. (Accessed 28 May 2017).
- Ohkubo, H., et al., 1997. Study on phase diagram of water ethanol solution. In: *Proc. of 18th Japan Symp. on Thermophysical Properties*, pp. 361–363.
- OIML, 1972. *International Alcoholometric Tables*. Available at: http://www.itecref.com/pdf/OIML_Alcoholometric_Tables.pdf.
- Ojeda, A., et al., 2017. Effect of process parameters on progressive freeze concentration of sucrose solutions. *Chem. Eng. Commun.*, 00986445.2017.1328413. Available at: <https://www.tandfonline.com/doi/full/10.1080/00986445.2017.1328413>. (Accessed 1 June 2017).
- Petzold, G., et al., 2016. Vacuum-assisted block freeze concentration applied to wine. *Innovat. Food Sci. Emerg. Technol.* 36, 330–335. Available at: <http://www.sciencedirect.com.ez.unisabana.edu.co/science/article/pii/S1466856416301515#s0010>. (Accessed 12 December 2017).
- Petzold, G., Aguilera, J.M., 2009. Ice morphology: fundamentals and technological applications in foods. *Food Biophys.* 4 (4), 378–396. Available at: <http://link.springer.com/10.1007/s11483-009-9136-5>. (Accessed 26 May 2015).
- Qin, F.G.F., Chen, X.D., Free, K., 2009. Freezing on subcooled surfaces, phenomena, modeling and applications. *Int. J. Heat Mass Tran.* 52 (5), 1245–1253. Available at: <http://www.sciencedirect.com.ez.unisabana.edu.co/science/article/pii/S0017931008005322>. (Accessed 10 April 2017).
- Raventós, M., et al., 2007. Concentration of aqueous sugar solutions in a multi-plate cryoconcentrator. *J. Food Eng.* 79 (2), 577–585. Available at: <http://www.sciencedirect.com.ez.unisabana.edu.co/science/article/pii/S0260877406001932>. (Accessed 15 May 2017).
- Robles, C.M., et al., 2016. Ice morphology modification and solute recovery improvement by heating and annealing during block freeze-concentration of coffee extracts. *J. Food Eng.* 189, 72–81. Available at: <http://www.sciencedirect.com.ez.unisabana.edu.co/science/article/pii/S0260877416301923>. (Accessed 25 January 2017).
- Sánchez, J., et al., 2011. Review: freeze concentration technology applied to dairy products. *Food Sci. Technol. Int.* 17 (1), 5–13. Available at: <http://fst.sagepub.com/cgi/doi/10.1177/1082013210382479>.
- Sánchez, J., et al., 2009. Review. Freeze concentration in the fruit juices industry. *Food Sci. Technol. Int.* 15 (4), 303–315.